INSTITUTE OF PHYSICS PUBLISHING SMART MATERIALS AND STRUCTURES
Smart Mater. Struct. **12** (2003) 881–888 PII: S0964-1726(03)67784-0

Mechanical description of interfacial slips for quartz crystal microbalances with viscoelastic liquid loading

F Lu, H P Lee[1] and S P Lim

Department of Mechanical Engineering, National University of Singapore,
9 Engineering Drive 1, 117576, Singapore

E-mail: hplee@ihpc.nus.edu.sg

Received 11 November 2002, in final form 17 July 2003
Published 30 September 2003
Online at stacks.iop.org/SMS/12/881

Abstract
Acoustic wave devices, such as quartz crystal microbalances (QCM), are extended to applications in liquid environments. An interfacial slip phenomenon is expected to occur at the interface between the surface of a quartz crystal sensor and the contacted liquid environment. Assumptions of continuous displacement and stress at the liquid–solid interface mask the physical details of the contact interface. In this paper, the motion equations of the interfacial particles are employed to replace the interfacial continuous displacement and continuous stress assumptions. The electrical impedance of QCM in the liquid environment is derived based on this proposed modeling. The comparison of the present result with that of the continuous stress and displacement model is presented. The slip parameter, which is defined as the amount of displacement transmission between the quartz crystal top surface and bottom liquid particles, is presented as a function of the contact properties. The effects of interactive force strength, liquid viscosity and attached-particles size are included in the numerical studies. The detailed modeling of the interface is useful in interpreting the slip phenomenon between the sensor surface and the liquid.

1. Introduction

Quartz crystal microbalances (QCM) provide a simple and effective means for detecting physical property changes of thin layers at their surfaces. Sauerbrey [1] first reported that a film attached to the surface of the electrodes of a piezoelectric quartz crystal resonator caused a decrease in the resonance frequency proportional to the mass of the film attached. The Sauerbrey equation is valid under the condition that the film is rigid and it is rigidly coupled to the oscillatory motion of the quartz crystal surface. One of the advantages of AT-cut QCM is their ability to act as a chemical detector in the liquid environment. After the discovery that the QCM resonator could also be used as a deposition monitor in liquids by Nomura [2], many studies were devoted to the behavior of QCM under complex liquid loading. When a QCM operates in a liquid environment, the oscillation of the device's surface is coupled into the liquid. The molecular layer attached to the QCM surface is neither rigidly coupled nor a simple Newtonian liquid. It has therefore become essential that models of the response of an acoustic device to the viscoelastic medium be developed.

The electrical analogue approaches [3], as well as the equivalent circuit of the resonating resonator and transmission line, have served effectively as methods for electrically characterizing the crystal. However, the analogue method often masks the physical insight into the detailed nature of the loading mechanism. The first acoustic wave analysis of a loaded resonator with elastic overlayer was performed by Miller and Bolef [4] and then simplified by Lu *et al* [5]. Reed *et al* [6] derived the electrical admittance of the QCM with a viscoelastic medium directly in terms of the physical properties of the compound resonator. Kanazawa [7]

[1] Address for correspondence: Institute of High Performance Computing, 1 Science Park Road, No. 01-01, The Capricorn Singapore Science Park II, 117528, Singapore.

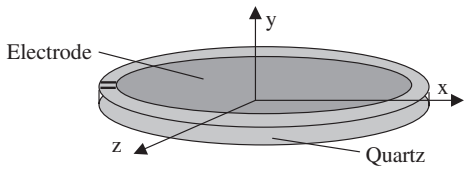

Figure 1. Quartz crystal resonator with electrodes on surface.

summarized the mechanical properties of QCM and overlayer correlating to the observed electrical behavior. A common feature of these treatments is that continuous shear stress and continuous displacement are assumed for the contact interface between the attached layer and sensor surface.

The role of interfacial slip between the sensor surface and the attached medium is one of the controversies in modeling the QCM liquid environment. Ferrante [8] defined the slip parameter as the ratio between the displacement of the liquid bottom surface and the displacement sensor contact surface and employed it to replace the continuous displacement assumption as the boundary condition for solving the equations. The slip friction force, which is proportional to the relative velocity between the contact surfaces, is employed by McHale [9] to analyze the interfacial slip influence.

In this paper, a detailed mechanical modeling of the contact interface for QCM operation in a liquid is proposed. The continuous displacement and stress assumption boundary conditions are replaced by the motion equations of contact molecules. The interface modeling includes the properties of the contact interface, such as attraction strength, contact molecular size and viscosity of the host liquid. The electrical admittance of QCM is derived directly in terms of mechanical properties. The slip parameter between the sensor surface and the liquid are evaluated as functions of the contact attraction strength and viscosity of the bulk liquid.

2. Quartz crystal microbalance with viscoelastic liquid loading

As shown in figure 1, the quartz crystal resonator is composed of a quartz crystal plate and two metal electrodes on its surfaces. To simplify the problem, the thickness of the electrode is neglected in the modeling. Changes in the properties of the liquid or in the surface mass density of the coating produce changes in the electrical impedance of the sensor. Normally, the quartz crystal is an AT-cut sample, with polarization axis y normal to the interface. When an electrical field is applied across the quartz crystal along the y direction, the mechanical displacement in the lateral direction is generated.

When the QCM is immersed in a liquid, the shear wave propagates into the liquid environment through the liquid–solid interface. The compound resonator is immersed in the liquid as shown in figure 2. The properties of the liquid and the contact conditions are reflected in the admittance spectrum of the QCM.

2.1. Motion equations of QCM with viscoelastic liquid loading

The QCM operates with the thickness shear vibration mode or its odd harmonics. Based on Newton's law, the wave equation of the piezoelectric resonator in the thickness shear mode can be expressed in the form [10]

$$\rho_{\mathrm{q}}\frac{\partial^2 u_{\mathrm{q}}}{\partial t^2} = \left(c_{66}^{\mathrm{q}} + \mathrm{j}\omega\eta_{\mathrm{q}} + \frac{e_{26}^2}{\epsilon_{22}}\right)\frac{\partial^2 u_{\mathrm{q}}}{\partial y^2}, \tag{1}$$

where u_{q} is the displacement in the lateral direction of the quartz element, ρ_{q} is the density of the quartz, c_{66}^{q} and e_{26} are the relevant elastic shear modulus and piezoelectric constant for the quartz crystal, ϵ_{22} is the dielectric constant, ω is the frequency and η_{q} is the viscosity of the quartz crystal. Comparing the equation with that for non-piezoelectric materials, the expression of the equivalent stiffness of the quartz has an extra term due to the electrical effect. The piezoelectric stiffness is defined as

$$\hat{c}_{\mathrm{q}} = c_{66}^{\mathrm{q}} + \mathrm{j}\omega\eta_{\mathrm{q}} + \frac{e_{26}^2}{\epsilon_{22}}. \tag{2}$$

The piezoelectric shear mode stiffness of the quartz $\hat{c}_{\mathrm{q}}$ is complex when the viscous loss is considered. In order to compare the Q factor of the unperturbed quartz and perturbed quartz, the tiny viscous loss of the quartz crystal is considered in this paper.

For a finite thickness slab of the resonator, because of wave reflection from the boundary, there are two waves in the slab. One of them propagates in the $+y$ direction and the other in the $-y$ direction. The solution of the motion equation (1) can be written as the sum of these two waves [11]:

$$u_{\mathrm{q}} = (A_1\mathrm{e}^{\mathrm{j}k_{\mathrm{q}}y} + B_1\mathrm{e}^{-\mathrm{j}k_{\mathrm{q}}y})\mathrm{e}^{\mathrm{j}\omega t}, \tag{3}$$

where A_1 and B_1 are constants determined by the boundary conditions and k_{q} is the shear wavevector within the quartz. From the constitutive relationship of the quartz crystal, the wavevector k_{q} is a function of the piezoelectric stiffness and its density, $\mathrm{j} = \sqrt{-1}$. The complex wave-propagating vector can be expressed as

$$k_{\mathrm{q}} = \omega\sqrt{\frac{\rho_{\mathrm{q}}}{\hat{c}_{\mathrm{q}}}}. \tag{4}$$

When the quartz resonator is working at the fundamental shear resonance frequency or its odd harmonics, the propagating vector is related to the thickness of the quartz resonator as

$$k_{\mathrm{q}} = \frac{2n+1}{h_{\mathrm{q}}}\pi \qquad n = 1, 2, 3, \ldots \tag{5}$$

where h_{q} is the thickness of the quartz crystal.

In order to determine the constants of the expression, the boundary conditions are needed, including the stress and displacement boundary conditions. The one-dimensional coupling constitutive relationship between the mechanical variables (stress and strain) and electrical variables (electric field and electric displacement) for piezoelectric materials for the relevant shear mode can be written as [10]

$$T_{\mathrm{q}} = c_{66}\gamma_{xy} + e_{26}E \tag{6a}$$

$$D_y = e_{26}\gamma_{xy} - \epsilon_{22}E, \tag{6b}$$

where the strain $\gamma_{xy} = \partial u_{\mathrm{q}}/\partial y$, T_{q} is the shear stress inside quartz, the electrical field E can be expressed as the differential

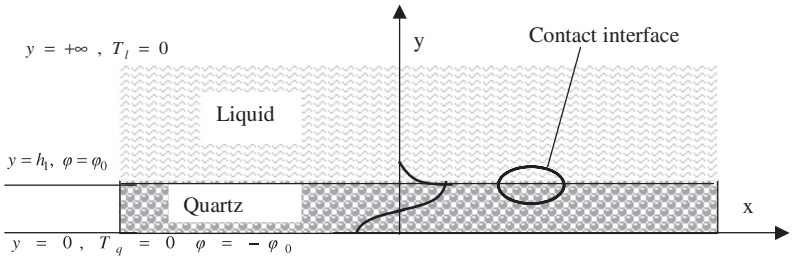

Figure 2. 2D schematic diagram of the QCM with semi-infinite liquid loading on the surface with boundary conditions.

form of the electric potential $E = \partial\phi/\partial y$ and D_y is the electrical displacement in the y direction. Associated with the one-dimensional electric displacement relation $\partial D_y/\partial y = 0$ and equation (6*b*), the relationship between the electrical potential and displacement can be expressed as

$$\epsilon_{22}\frac{\partial^2\phi}{\partial y^2} - e_{26}\frac{\partial^2 u_\mathrm{q}}{\partial y^2} = 0. \tag{7}$$

The electrical potential ϕ is given as follows:

$$\phi(y,t) = \left(\frac{e_{26}}{\epsilon_{22}}A_1 \mathrm{e}^{\mathrm{j}k_\mathrm{q}y} + \frac{e_{26}}{\epsilon_{22}}B_1\mathrm{e}^{-\mathrm{j}k_\mathrm{q}y} + Cy + D\right)\mathrm{e}^{\mathrm{j}\omega t} \tag{8}$$

where C and D are constants to be determined by the boundary conditions. Substituting the expressions of strain and electrical field into equation (6*a*), the shear stress inside the quartz crystal can be easily expressed as

$$T_\mathrm{q} = \mathrm{j}\hat{c}_\mathrm{q}k_\mathrm{q}(A_1\mathrm{e}^{\mathrm{j}k_\mathrm{q}y} - B_1\mathrm{e}^{-\mathrm{j}k_\mathrm{q}y})\mathrm{e}^{\mathrm{j}\omega t} + Ce_{26}E\mathrm{e}^{\mathrm{j}\omega t}. \tag{9}$$

The equations of motion for the liquid medium are expressed as a combination of the continuity equations, Hooke's law and Newton's second law [12]:

$$\rho_\mathrm{v} + (\rho_\mathrm{v}u_i')_i = 0 \tag{10}$$

$$(T_\mathrm{v})_{ij} = -p_\mathrm{v}\delta_{ij} + \eta_\mathrm{l}(u_{i,j}' + u_{j,i}') + (\xi - 0.67\eta_\mathrm{v})\delta_{ij}u_{k,k}' \tag{11}$$

$$(T_\mathrm{v})_{ij,i} + F_j = \rho_\mathrm{v}(u_j'' + u_i'u_{j,i}'). \tag{12}$$

The general solution of the expressions for motion for a damped plane wave propagating in the liquid environment was obtained by Ferrante *et al* [8], assuming incompressible flow, no external forces, constant viscosity and neglecting the non-linear term of the displacement. Their expression for the liquid displacement and shear stress are similarly expressed as

$$u_\mathrm{v} = (A_2\mathrm{e}^{\mathrm{j}k_\mathrm{v}y} + B_2\mathrm{e}^{-\mathrm{j}k_\mathrm{v}y})\mathrm{e}^{\mathrm{j}\omega t} \tag{13}$$

$$T_\mathrm{v} = \mathrm{j}\hat{c}_\mathrm{v}k_\mathrm{v}(A_2\mathrm{e}^{\mathrm{j}k_\mathrm{v}y} - B_2\mathrm{e}^{-\mathrm{j}k_\mathrm{v}y})\mathrm{e}^{\mathrm{j}\omega t} \tag{14}$$

where $\hat{c}_\mathrm{v} = c_{66}^\mathrm{v}+\mathrm{j}\omega\eta_\mathrm{v}$, with c_{66}^v and η_v as the shear modulus and viscosity of the viscoelastic liquid and $k_\mathrm{v} = \omega\sqrt{\rho_\mathrm{v}/\hat{c}_\mathrm{v}}$, with ρ_v the density of the viscoelastic liquid. A_2, B_2 are complex constants to be determined by the boundary conditions. There are six undetermined constants to be derived from the boundary conditions. In order to describe the physical behavior of the quartz and the layer, six independent boundary conditions are needed. The problem is focused on solving the unknown constants in the above expressions according to the boundary conditions.

The wave displacement generates an accompanying electrical potential through which the piezoelectric wave can be electrically detected. The impedance/admittance analysis, in which the spectrum of the impedance/admittance of the compound sensor is recorded as a function of the excitation frequency, is widely used to detect the perturbation of the BAW sensors. The admittance is defined as the ratio of the input current to the voltage. The explicit expression of the current of the piezoelectric materials is $Q = \int_{\bar{A}} D_2\,\mathrm{d}A$ [12]. The current across the quartz crystal, which is the time derivative of the charge, can be expressed as

$$I = -\mathrm{j}\omega\epsilon_{22}C\bar{A} \tag{15}$$

where $\bar{A}$ is the effective electrode surface area and C is the constant from equation (8). The admittance of the quartz crystal resonator can be determined as

$$Y = \frac{I}{V} = \frac{\mathrm{j}\omega\epsilon_{22}\bar{A}}{2\varphi_0}C. \tag{16}$$

After the constant C is determined from the boundary conditions, the spectrum of the admittance can be predicted. The expression of equation (16) is a common expression for the admittance of a quartz crystal resonator with multi-layer loading.

2.2. Mechanical description of the interface boundary conditions

In order to solve the motion equations in section 2.1, six boundary conditions are needed. At the interface between the quartz crystal surface and the viscoelastic molecular layer, the transverse vibratory motion of particles at the top of the crystal surface causes the transverse motion of the particles of the attached layer in contact with the sensor surface. The transverse shear wave is partially transmitted and partially reflected. The amount of transmission and reflection depends on the physical and chemical properties of the interface and the attached viscoelastic layers. The continuous displacement and stress assumptions mask the detailed mechanical behavior of the contact interface.

The interfacial slip between the quartz surface and layer is modeled as a local molecular mass and interaction element between the masses, as shown in figure 3. The m_1 represents the mass particle on the layer surface and m_2 represents the mass particle on the quartz surface. Both displacements of the mass particles are restricted to the x direction. The interaction between the two particles is presented as a spring and damper with complex parameters G^*, which is the force when

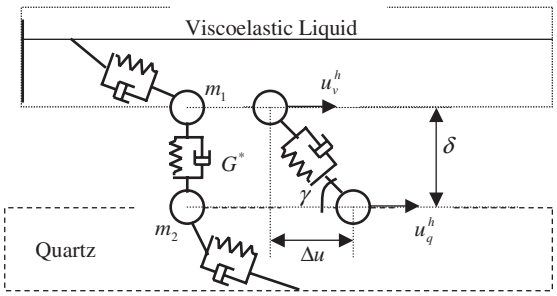

Figure 3. Mechanical description of the contact interface between the liquid and the sensor surface.

unit shear displacement occurs between two contact particles. Besides the interaction force from the sensor surface particles, there are internal attraction forces from the bulk liquid. This interaction is proportional to the gradient of the displacement in the x direction. The interaction force between the two contact surfaces molecules is modeled as the spring-dashpot force, which is proportional to the relative displacement/velocity between the molecules of the two surfaces. The shear force on the interface is equal to the spring force plus the damping force.

In this paper, discussions are focused on the AT-cut thickness shear mode resonator. Therefore, only the shear deformation and thickness shear stresses are considered. To extend to other acoustic sensors, such as SAW, PLE, etc, the corresponding deformation and stress are needed to replace the shear components here.

The lateral displacement of the quartz contact surface molecules is noted as u_{q}^h and the displacement of the contact particles at the bottom of the liquid is denoted as u_{v}^h. The relative displacement in the x direction can be expressed as $\Delta u = u_{\mathrm{q}}^h - u_{\mathrm{v}}^h$. The interactive force is proportional to the relative shear displacement. This assumption is valid when the relative deformation is small, which is within the linear elastic region. The equivalent shear deformation of the interface can be expressed as

$$\gamma = \frac{\Delta u}{\delta} = \frac{u_{\mathrm{q}}^h}{\delta} - \frac{u_{\mathrm{v}}^h}{\delta} \tag{17}$$

where δ is the distance between the molecules on the quartz surface and those on the viscoelastic layer contact surface, as illustrated in figure 3. The force keeping the connection between the two contact surfaces is like the shear stress on the continuous medium. The interactive force can be expressed as

$$F = G^*\gamma = G'\gamma + G''\dot{\gamma} = (G' + \mathrm{j}\omega G'')\left(\frac{u_{\mathrm{q}}^h}{\delta} - \frac{u_{\mathrm{v}}^h}{\delta}\right). \tag{18}$$

The single shear vibration mode is considered in the QCM compound resonator, where the particles on the surface have the same vibration phase. The model is reduced to a one-dimensional problem. Based on Newton's law, the motion equation of the particles on the viscoelastic layer surface can be expressed as

$$\rho_{\mathrm{v}}\Delta_{\mathrm{v}}\ddot{u}_{\mathrm{v}}^h + T_{\mathrm{v}}^h + \frac{G^*}{\delta}(u_{\mathrm{q}}^h - u_{\mathrm{v}}^h) = 0 \tag{19}$$

where $(\bullet)^h$ means the corresponding value on the interfacial layer. ρ_{v} is the density of the molecular layer, $G^* = G' + \mathrm{j}\omega G''$ is the equivalent shear stiffness of the interfacial connection between the quartz surface and the viscoelastic layer, with G' as the storage stiffness and G'' as the dissipated stiffness, Δ_{v} represents the height of the molecular layer attached to the sensor surface, u_{v}^h and u_{q}^h are lateral displacements of the attached molecules and quartz surface, respectively. and T_{v}^h is the shear stress on the bottom of the liquid in contact with the sensor surface having $y = h_1$:

$$T_{\mathrm{v}}^h = \mathrm{j}\hat{c}_{\mathrm{v}}k_{\mathrm{v}}(A_2\mathrm{e}^{\mathrm{j}k_{\mathrm{v}}h_1} - B_2\mathrm{e}^{-\mathrm{j}k_{\mathrm{v}}h_1})\mathrm{e}^{\mathrm{j}\omega t}. \tag{20}$$

Substituting the expression for the displacements of the quartz crystal and the liquid medium (equations (3), (13) and (20)) into equation (19) we get

$$\begin{aligned}&\frac{G^*}{\delta}\mathrm{e}^{\mathrm{j}k_{\mathrm{q}}h_1}A_1 + \frac{G^*}{\delta}\mathrm{e}^{-\mathrm{j}k_{\mathrm{q}}h_1}B_1\\ &\quad + \left[-\rho_{\mathrm{v}}\Delta_{\mathrm{v}}\omega^2 + \mathrm{j}c_{\mathrm{v}}k_{\mathrm{v}} - \frac{G^*}{\delta}\right]\mathrm{e}^{\mathrm{j}k_{\mathrm{v}}h_2}A_2\\ &\quad + \left[-\rho_{\mathrm{v}}\Delta_{\mathrm{v}}\omega^2 - \mathrm{j}c_{\mathrm{v}}k_{\mathrm{v}} - \frac{G^*}{\delta}\right]\mathrm{e}^{-\mathrm{j}k_{\mathrm{v}}h_1}B_2 = 0.\end{aligned} \tag{21}$$

With the same consideration given to quartz crystal particles at the top of the quartz resonator, another boundary condition on the interface between the quartz crystal surface and the attached layer can be expressed as

$$\begin{aligned}&\left[-\rho_{\mathrm{q}}\Delta_{\mathrm{q}}\omega^2 + \mathrm{j}c_{\mathrm{q}}k_{\mathrm{q}} + \frac{G^*}{\delta}\right]\mathrm{e}^{\mathrm{j}k_{\mathrm{v}}h_1}A_1\\ &\quad + \left[-\rho_{\mathrm{q}}\Delta_{\mathrm{q}}\omega^2 - \mathrm{j}c_{\mathrm{q}}k_{\mathrm{q}} + \frac{G^*}{\delta}\right]\mathrm{e}^{-\mathrm{j}k_{\mathrm{v}}h_1}B_1\\ &= \frac{G^*}{\delta}\mathrm{e}^{\mathrm{j}k_{\mathrm{v}}h_1}A_2 + \frac{G^*}{\delta}\mathrm{e}^{-\mathrm{j}k_{\mathrm{v}}h_1}B_2 + e_{26}C.\end{aligned} \tag{22}$$

Combining equations (21) and (22), and canceling the interactive force between the two surfaces, the boundary condition expression (22) can be replaced by

$$\begin{aligned}&[-\rho_{\mathrm{q}}\Delta_{\mathrm{q}}\omega^2 + \mathrm{j}c_{\mathrm{q}}k_{\mathrm{q}}]\mathrm{e}^{\mathrm{j}k_{\mathrm{v}}h_1}A_1\\ &\quad + [-\rho_{\mathrm{q}}\Delta_{\mathrm{q}}\omega^2 - \mathrm{j}c_{\mathrm{q}}k_{\mathrm{q}}]\mathrm{e}^{-\mathrm{j}k_{\mathrm{v}}h_1}B_1 + e_{26}C\\ &= [-\rho_{\mathrm{v}}\Delta_{\mathrm{v}}\omega^2 + \mathrm{j}c_{\mathrm{v}}k_{\mathrm{v}}]\mathrm{e}^{\mathrm{j}k_{\mathrm{v}}h_1}A_2\\ &\quad + [-\rho_{\mathrm{v}}\Delta_{\mathrm{v}}\omega^2 - \mathrm{j}c_{\mathrm{v}}k_{\mathrm{v}}]B_2.\end{aligned} \tag{23}$$

The continuous displacement assumption and continuous stress assumption on the interface are replaced by the more detailed description of the contact interfacial properties.

When the inertia of the contact particles' mass is small enough, and the effect of inertia is neglected, equation (23) is reduced to the equation for continuous stress assumption [9]:

$$\begin{aligned}&\mathrm{j}c_{\mathrm{q}}k_{\mathrm{q}}\mathrm{e}^{\mathrm{j}k_{\mathrm{v}}h_1}A_1 - \mathrm{j}c_{\mathrm{q}}k_{\mathrm{q}}\mathrm{e}^{-\mathrm{j}k_{\mathrm{v}}h_1}B_1 + e_{26}C\\ &= \mathrm{j}c_{\mathrm{v}}k_{\mathrm{v}}\mathrm{e}^{\mathrm{j}k_{\mathrm{v}}h_1}A_2 - \mathrm{j}c_{\mathrm{v}}k_{\mathrm{v}}\mathrm{e}^{-\mathrm{j}k_{\mathrm{v}}h_1}B_2.\end{aligned} \tag{24}$$

Furthermore, when the contact interactive force is much larger, that is, the shear stiffness between the two contact interfaces is much higher than that of the contact viscoelastic layer, equation (21) can be reduced to the continuous displacement assumption [7]:

$$\frac{G^*}{\delta}\mathrm{e}^{\mathrm{j}k_{\mathrm{q}}h_1}A_1 + \frac{G^*}{\delta}\mathrm{e}^{-\mathrm{j}k_{\mathrm{q}}h_1}B_1 - \frac{G^*}{\delta}\mathrm{e}^{\mathrm{j}k_{\mathrm{v}}h_2}A_2 - \frac{G^*}{\delta}\mathrm{e}^{-\mathrm{j}k_{\mathrm{v}}h_1}B_2 = 0. \tag{25}$$

Table 1. Parameters of a quartz crystal microbalance for analysis.

Quartz parameters	Value	Description
ρ_q	2649 kg m^{-3}	Density
c_q	2.91×10^{10} N m^{-2}	Shear modulus
e_{26}	7.98×10^{-2} C m^{-2}	Piezoelectric constant
ϵ_{22}	3.982×10^{-11} C V^{-1} m^{-1}	Permittivity
η_q	8.376×10^{-3} N s m^{-1}	Effective viscosity of quartz crystal
$\bar{A}$	0.2984 cm^2	Effective electrode surface area

Now, combining equations (21) and (23) the boundary conditions illustrated in figure 2 are

$$y = +\infty, \qquad u_v = 0 \Rightarrow A_2 = 0 \tag{26}$$

$$y = h_1,$$

$$\varphi(h_1) = \varphi_0 \Rightarrow \frac{e_{26}}{\epsilon_{22}}(A_1 e^{jk_q h_1} + B_1 e^{-jk_q h_1}) + h_1 C + D = \varphi_0 \tag{27}$$

$$y = 0, \qquad T_q(h_1) = 0 \Rightarrow j\hat{c}_q k_q (A_1 - B_1) + e_{26} C = 0 \tag{28}$$

$$y = 0, \qquad \varphi(h_1) = -\varphi_0 \Rightarrow \frac{e_{26}}{\epsilon_{22}}(A_1 + B_1) + D = -\varphi_0 \tag{29}$$

where φ_0 is the electrical potential applied at the upper electrode. Constants A_1, B_1, A_2, B_2, C and D can be solved based on six equations. The expressions of these constants are given in the appendix.

The ratio between the complex displacement of liquid bottom particles and the sensor surface displacement is defined as the slip parameter by Ferrante [12]:

$$\alpha = \frac{u_v^h}{u_q^h}. \tag{30}$$

Based on the mechanical modeling, the slip parameter can be expressed as

$$\alpha = \frac{A_2 e^{jk_v h_1} + B_2 e^{-jk_v h_1}}{A_1 e^{jk_q h_1} + B_1 e^{-jk_q h_1}} = \frac{A_2}{A_1 e^{j(kq - k_v)h_1} + B_1 e^{-(k_q + k_v)h_1}}. \tag{31}$$

3. Results and discussions

3.1. QCM model for numerical analysis

The same parameters for the QCM presented in [8] are used in this study. The parameters of the quartz crystal are summarized in table 1.

The admittance and impedance spectrum of the QCM under air without external loading evaluated from the equations are illustrated in figures 4 and 5. The resonance frequency and anti-resonance frequency of the first shear mode vibration are 9.0039 and 9.023 28 MHz, respectively. Because of its lower viscoelastic coefficient, unperturbed QCM under the air condition is considerably sharper for the admittance phase and magnitude curves. With the viscoelastic layer attached to the sensor surface, the sharpness of the spectrum is more rounded due to the decreasing Q factor, besides the frequency shift.

In this paper, the mass attached to the sensor surface is assumed to be uniform on the surface. The roughness of the quartz surface is neglected as well. The sensitivity of the frequency as the mass changes can be described as the ratio between the frequency shift Δf and the layer height Δh_v:

$$S_f = \frac{\Delta f}{\Delta m} = \frac{\Delta f}{\rho_v \bar{A} \Delta h_v} \tag{32}$$

where ρ_v is the density of the attached mass. The Sauerbrey equation presented a linear relationship between the frequency shift and the attached mass [1], i.e. the mass sensitivity S_f is constant. The linear relationship of the Sauerbrey equation is only applicable for thin absorption layers. Under the non-slip assumption with an elastic mass layer, figure 6 gives the frequency shift versus the thickness of the attached layer, in which the density of the layer is $\rho_v = 1000$ kg m^{-3}. The x coordinate is the ratio between the thickness of the attached layer and that of the quartz resonator. The linear ratio between the frequency shift and the thickness of the attached layer is valid for the small region. When the thickness of the attached layer is beyond 6% of the quartz thickness, the mass sensitivity of the elastic layer is obviously different from that derived from the Sauerbrey equation. As the elastic shear modulus of the attached layer decreases, this nonlinearity is more serious as illustrated in figure 6.

When the QCM is immersed in the viscoelastic liquid environment, its admittance spectrum sharpness is changed as well as the resonance frequency shift. Bold curves in figures 7 and 8 give the amplitude and phase plot of the QCM in a typical liquid environment, in which the viscosity of the liquid is set as $\eta_v = 0.05$ N s m^{-2} and the shear storage stiffness is set as $c_v = 10$ N m^{-2}. The tiny shear storage stiffness of the liquid prevents the wave from propagating into the liquid and then the wave is attenuated rapidly in the liquid. The liquid

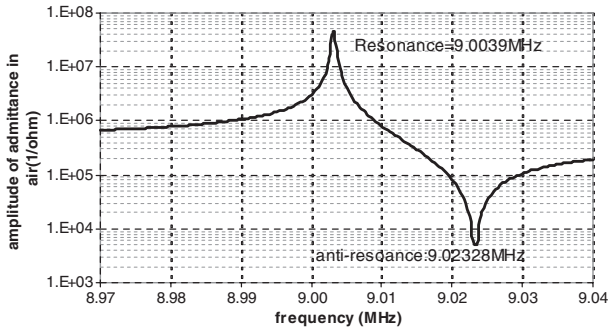

Figure 4. Amplitude of the admittance spectrum of QCM in air (without loading).

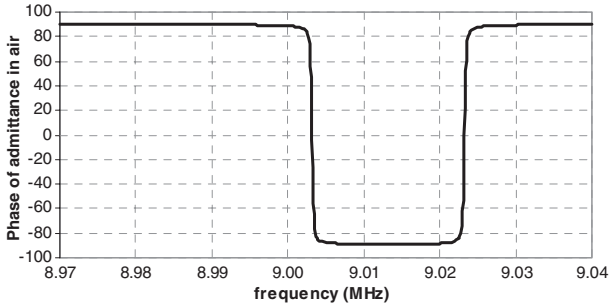

Figure 5. Phase of the admittance spectrum of QCM in air (without loading).

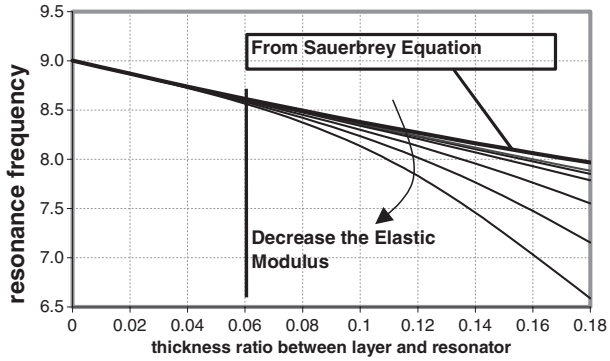

Figure 6. Resonance frequency of the QCM with different thicknesses of elastic mass layer.

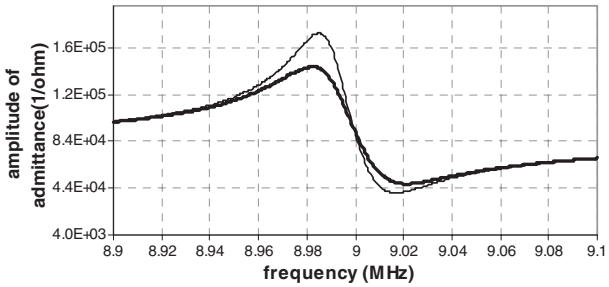

Figure 7. Amplitudes of admittances of the QCM in liquid for the proposed modeling and the non-slip modeling (bold curve—current modeling, normal curve—non-slip modeling).

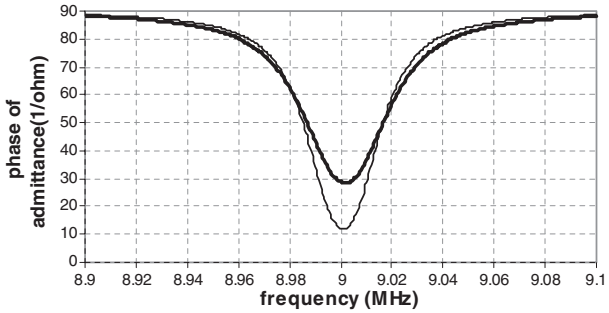

Figure 8. Phase of admittance of the QCM in liquid for the proposed modeling and the non-slip modeling (bold curve—current modeling, normal curve—non-slip modeling).

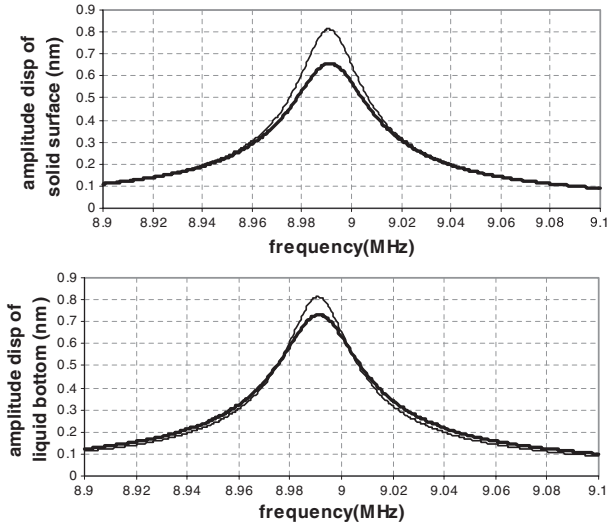

Figure 9. Displacements of the contact interface layers for the proposed modeling and non-slip modeling (bold curve—current modeling, normal curve—non-slip modeling).

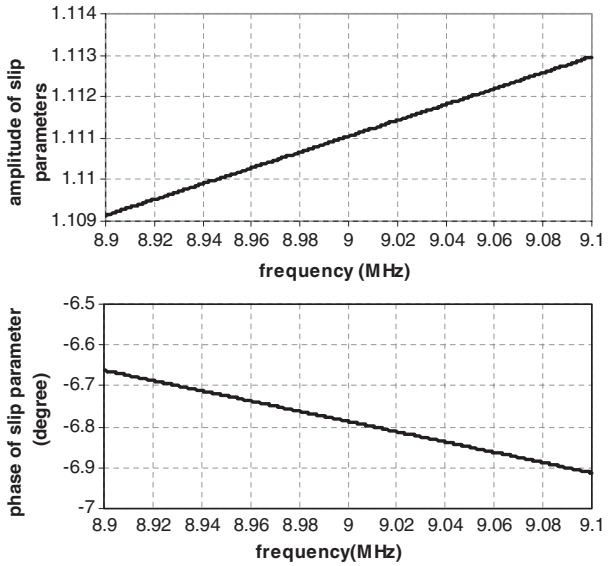

Figure 10. Amplitude and phase of the slip parameter.

is assumed to be semi-infinite and there is no reflecting shear wave from the surface of the liquid. The distance between the two contact layers of the liquid and the quartz surface is set as $\delta = 1.5 \times 10^{-10}$ m. The resonance frequency of the QCM is reduced due to the liquid loading and its admittance spectrum sharpness is more rounded. The displacement spectra of the sensor surface and that of the bottom of the liquid are presented as bold curves in figure 9. The slip parameter as a function of frequency around the QCM shear resonance is presented in figure 10. The amplitude of the slip parameter at the QCM resonance frequency of 8.993 MHz is 1.11 and the corresponding phase is $-6.78°$. The displacement of the sensor surface is partially transmitted into the liquid particles.

The results evaluated from the non-slip models are presented in figures 7 and 8, which are plotted as normal curves. Comparing with the results of the slip model, the Q factor of the QCM which is evaluated from the non-slip model is larger than that evaluated from the slip model. The displacement of the sensor surface and the displacement of the liquid bottom surface are also presented in figure 9. The ratio between these displacements is defined as the slip parameter. The difference between these two modes is that the inertia effect and the phase changes between the two contact interfaces are included. It is intuitive that, with increasing strength of the interactive force and reducing the molecular size, results evaluated from the mechanical mode in this paper is close to that of the non-slip model.

The slip parameter on the interface reflects the vibration transmission between the sensor surface particles and liquid particles. It is dependent on the contact properties of the interface. The interactive force between the liquid molecules and the sensor surface, the liquid molecular size attached to the surface and the viscosity of the host liquid environment

affect the QCM performance. The relationship between the slip parameter and the mechanical properties can be used to measure the behavior of the solid–liquid interface.

3.2. Study of the contact condition parameters for the QCM in liquid

The resonance frequency and the Q factor of the QCM electrical admittance respond to changes in the contact conditions as well as to the properties of the bulk liquid. The model derived from the continuous stress and continuous displacement assumptions masks the detailed mechanical properties of the contact interface. As illustrated in equation (26), the interfacial slip phenomena are described by the transfer function between the displacements of particles at the top of the sensor surface and that of particles at the bottom of the attached layer in contact with the sensor. The local spring–damper-mass model proposed in this paper is an attempt for a detailed evaluation of the phenomena at the interfacial layer. By coating different biological layers on the QCM surface, the interactive force between the sensor's surface and the attached molecular particles can be changed, for example by using hydrophilic- or hydrophobic-coated sensors. In addition, the contact condition is also affected by the size of the attached molecules and the properties of the host liquid. The corresponding parameters for these contact conditions are included in the modeling equations (21) and (23).

The amplitude of the slip parameter $|\alpha|$ and its phase as functions of the interactive force strength modulus G' are plotted in figures 11 and 12. The amplitude of the slip parameter approaches one and the phase approaches zero as the strength of the interactive force increases. There is a peak value for the slip parameter amplitude at certain values of the strength of the interactive force. This is due to the fact that coupling resonance happens between the contact particle pairs. The value of the interactive strength, which gives the maximum amplitude of the slip parameter, depends on the viscosity of the bulk liquid. Higher liquid viscosity shifts the peak of the slip parameter to the left, as shown in figure 11. When the interactive strength is smaller than the value which gives the local resonance, higher viscosity results in a smaller amplitude for the slip parameter. This trend is in agreement with the experimental results reported by Ferrante [8] that slip parameter decreases and approaches unity as the liquid viscosity increases. The reverse trend exists for the slip parameter as a function of the liquid viscosity when the attraction strength is larger than the value, which results in local resonance.

Keeping the interactive strength constant at $G' = 300$ Pa, which is smaller than the value corresponding to the maximum slip parameter, and changing the liquid viscosity, the slip parameter as a function of the liquid viscosity is plotted in figure 13. The slip parameter decreases as the viscosity of the bulk liquid increases. However, with the higher value of the interface interactive strength, the relationship between the slip parameter and the liquid viscosity are different. As shown in figure 14, the interactive strength value is set as $G' = 5000$ Pa, which is larger than the value corresponding to the maximum slip parameter. The amplitude of the slip parameter increases as the viscosity of the bulk liquid increases.

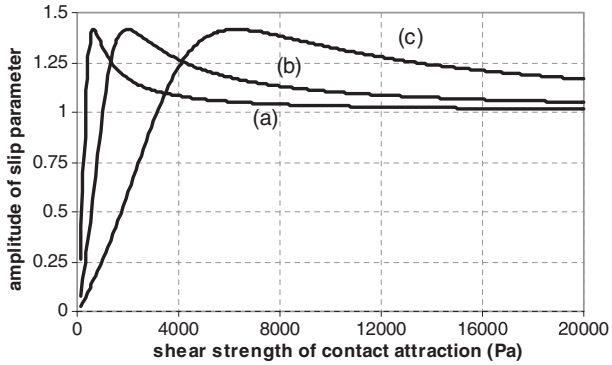

Figure 11. Amplitude of the slip parameter $|\alpha(\omega)|$ as a function of the viscosity of the bulk liquid: (a) liquid viscosity $= 0.05$ N s m^{-3}, (b) liquid viscosity $= 0.5$ N s m^{-3} and (c) liquid viscosity $= 5$ N s m^{-3}.

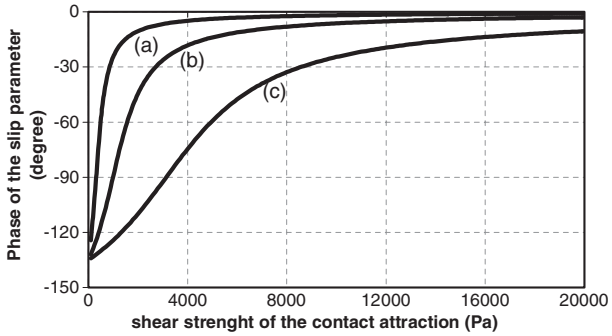

Figure 12. Phase of the slip parameter as a function of viscosity of the bulk liquid: (a) liquid viscosity $= 0.05$ N s m^{-3}, (b) liquid viscosity $= 0.5$ N s m^{-3} and (c) liquid viscosity $= 5$ N s m^{-3}.

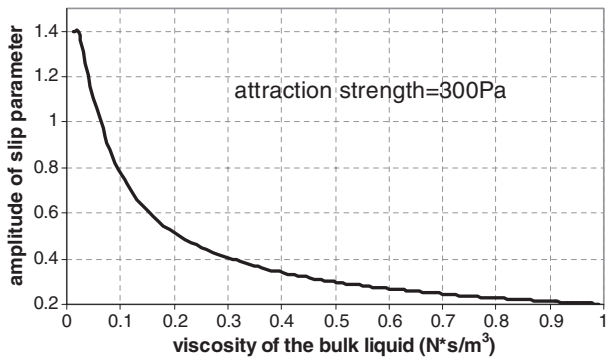

Figure 13. Amplitude of the slip parameter versus viscosity of the liquid with attraction strength $= 300$ Pa.

From the simulation results, it is shown that the slip parameter is not linearly proportional to the liquid viscosity, and the changing trend of the amplitude of the slip parameter as a function of liquid viscosity varies with different interface interactive forces.

4. Conclusions

The continuous stress and continuous displacement assumptions were employed for application of the QCM in air condition. However, the assumptions at the interface mask the mechanical properties of the contact conditions. The error due

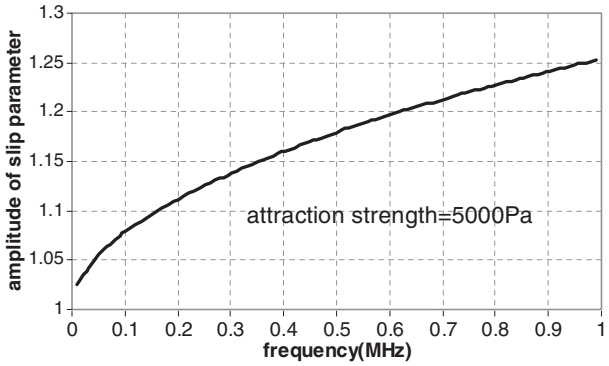

Figure 14. Amplitude of the slip parameter versus viscosity of the liquid with attraction strength = 5000 Pa.

to the non-slip assumptions cannot be ignored when the QCM operates in the low viscosity liquid environment. In this paper, a detailed mechanical modeling of the interface layer is proposed, which involves the properties of the contact interface, such as the interactive strength, contact molecular size and the viscosity of the liquid. The motion equations of the contact particles are employed to replace the continuous stress and displacement assumptions at the interface. The numerical results are compared with the results evaluated from the non-slip model. The amplitude evaluated from the model in this paper is smaller than that evaluated from the non-slip model. By numerical analysis, the slip parameter is studied. There is an interactive strength value that gives the maximum amplitude of the slip parameter. The slip parameter of the contact interface evaluated from the model is a function of the interactive strength and viscosity of the bulk liquid. By measuring the slip parameter of the contact interface, the changes in the attraction strength and liquid properties can be determined. The detailed mechanical description of the solid–liquid interface of the QCM in a liquid provides an approach to understanding the performance of the QCM description of the interface in a liquid and it is useful for exploring fresh ideas for the use of AT-cut quartz crystals.

Appendix. Expressions of the constants A_1, B_1, A_2, B_2, C, D by solving the six boundary conditions.

$$A_1 = \{2P_2\varphi_0\}\left\{\left(\frac{e_{26}}{\epsilon_{22}}e^{jk_qh_1} - \frac{e_{26}}{\epsilon_{22}} - j\frac{h_1}{e_{26}}\hat{c}_qk_q\right)P_2 + \left(\frac{e_{26}}{\epsilon_{22}}e^{-jk_qh_1} - \frac{e_{26}}{\epsilon_{22}} + j\frac{h_1}{e_{26}}\hat{c}_qk_q\right)P_1\right\}^{-1}$$

$$B_1 = \{2P_1\varphi_0\}\left\{\left(\frac{e_{26}}{\epsilon_{22}}e^{jk_qh_1} - \frac{e_{26}}{\epsilon_{22}} - j\frac{h_1}{e_{26}}\hat{c}_qk_q\right)P_2 + \left(\frac{e_{26}}{\epsilon_{22}}e^{-jk_qh_1} - \frac{e_{26}}{\epsilon_{22}} + j\frac{h_1}{e_{26}}\hat{c}_qk_q\right)P_1\right\}^{-1}$$

$$A_2 = 0$$

$$B_2 = \frac{\frac{G^*}{\delta}e^{jk_2h_1}}{j\hat{c}_vk_v + \frac{G^*}{\delta} + \rho_v\Delta_v\omega^2}\{2(e^{jk_qh_1}P_2 + e^{-jk_qh_1}P_1)\varphi_0\} \times \left\{\left(\frac{e_{26}}{\epsilon_{22}}e^{jk_qh_1} - \frac{e_{26}}{\epsilon_{22}} - j\frac{h_1}{e_{26}}\hat{c}_qk_q\right)P_2 + \left(\frac{e_{26}}{\epsilon_{22}}e^{-jk_qh_1} - \frac{e_{26}}{\epsilon_{22}} + j\frac{h_1}{e_{26}}\hat{c}_qk_q\right)P_1\right\}^{-1}$$

$$C = \frac{2j\hat{c}_qk_q\varphi_0}{e_{26}} \times \left[\{P_1 - P_2\}\left\{\left(\frac{e_{26}}{\epsilon_{22}}e^{jk_qh_1} - \frac{e_{26}}{\epsilon_{22}} - j\frac{h_1}{e_{26}}\hat{c}_qk_q\right)P_2 + \left(\frac{e_{26}}{\epsilon_{22}}e^{-jk_qh_1} - \frac{e_{26}}{\epsilon_{22}} + j\frac{h_1}{e_{26}}\hat{c}_qk_q\right)P_1\right\}^{-1}\right]$$

$$D = -\varphi_0 - \frac{2e_{26}\varphi_0}{\epsilon_{22}} \left[\{P_1 + P_2\}\left\{\left(\frac{e_{26}}{\epsilon_{22}}e^{jk_qh_1} - \frac{e_{26}}{\epsilon_{22}} - j\frac{h_1}{e_{26}}\hat{c}_qk_q\right)P_2 + \left(\frac{e_{26}}{\epsilon_{22}}e^{-jk_qh_1} - \frac{e_{26}}{\epsilon_{22}} + j\frac{h_1}{e_{26}}\hat{c}_qk_q\right)P_1\right\}^{-1}\right]$$

where

$$P_1 = [(j\hat{c}_qk_q + \rho_q\Delta_q\omega^2)e^{2jk_qh_1} - j\hat{c}_qk_qe^{jk_qh_1}] \times \left(j\hat{c}_vk_v + \frac{G^*}{\delta} + \rho_v\Delta_v\omega^2\right) + e^{2jk_qh_1}\frac{G^*}{\delta}(j\hat{c}_vk_v + \rho_v\Delta_v\omega^2)$$

$$P_2 = (j\hat{c}_qk_q + \rho_q\Delta_q\omega^2 - j\hat{c}_qk_qe^{jk_qh_1}) \times \left(j\hat{c}_vk_v + \frac{G^*}{\delta} + \rho_v\Delta_v\omega^2\right) - \frac{G^*}{\delta}(j\hat{c}_vk_v + \rho_v\Delta_v\omega^2).$$

References

[1] Sauerbrey G 1959 Verwendung von schwingquarzen zur wagung dunner schechten and zur mikrowagung *Z. Phys.* **155** 206–22

[2] Nomura T and Okugara M 1982 Frequency shifts of piezoelectric quartz crystals immersed in organic liquids *Anal. Chim. Acta* **142** 281–4

[3] Cernosek R W, Martin S J, Hillman A R and Bandey H L 1998 Comparison of lumped-element and transmission-line models for thickness-shear-mode quartz resonator sensors *IEEE Trans. Ultrason. Ferroelectr. Freq. Control* **45** 1399–407

[4] Miller J G and Bolef D I 1968 Sensitivity enhancement by the use of acoustic resonators in cw ultrasonic spectroscopy *J. Appl. Phys.* **39** 4589–93

[5] Lu C S and Lewis O 1972 Investigation of film-thickness determination by oscillating quartz resonators with large mass load *J. Appl. Phys.* **43** 4385–90

[6] Reed C E, Kanazawa K K and Kaufman J H 1990 Physical description of a viscoelastically loaded AT-cut quartz resonator *J. Appl. Phys.* **68** 1993–2001

[7] Kanazawa K K 1997 Mechanical behaviour of films on the quartz microbalance *Faraday Discuss.* **107** 77–90

[8] Ferrante F, Kipling A L and Thompson M 1994 Molecular slip at the solid–liquid interface of an acoustic-wave sensor *J. Appl. Phys.* **76** 3448–62

[9] McHale G, Lucklum R, Newton M I and Cowen J A 2000 Influence of viscoelasticity and interfacial slip on acoustic wave sensors *J. Appl. Phys.* **88** 7304–12

[10] Ballantine D S, White R M Jr, Martin S J, Ricco A J, Frye G C, Zellers E T and Wohltjen H 1997 *Acoustic Wave Sensors: Theory, Design and Physico-Chemical Application* (New York: Academic)

[11] Rosenbaum J F 1988 *Bulk Acoustic Wave Theory and Devices* (Boston, MA: Artech House Publishers) chapter 5

[12] Zelenka J 1986 *Piezoelectric Resonators and the Applications* (Amsterdam: Elsevier)